ton blooms due to excessive nutrient influxes; if unchecked, such conditions can deplete the oxygen content of the water and result in massive fish kills. The link between ocean color and phytoplankton concentration afforded by the Nimbus-7 CZCS offers an important and exciting new observational tool.

W. A. HOVIS
D. K. CLARK
National Environmental Satellite Service, National Oceanic and Atmospheric Administration, Washington, D.C. 20233
F. ANDERSON
National Research Institute for Oceanology, Cape Town, South Africa
R. W. AUSTIN
W. H. WILSON
Visibility Laboratory, Scripps Institution of Oceanography, San Diego, California 92152
E. T. BAKER
Pacific Marine Environmental Laboratory, National Oceanic and Atmospheric Administration, Seattle, Washington 98105
D. BALL
Computer Sciences Corporation, Silver Spring, Maryland 20910
H. R. GORDON
Department of Physics, University of Miami, Coral Gables, Florida 33124
J. L. MUELLER
Laboratory for Atmospheric Sciences, National Aeronautics and Space Administration, Goddard Space Flight Center, Greenbelt, Maryland 20771
S.Z. EL-SAYED
Texas A&M University, College Station 77843
B. STURM
Commission of the European Communities, Joint Research Center, Ispra Establishment, 21020 Ispra, Italy
R. C. WRIGLEY
National Aeronatics and Space Administration, Ames Research Center, Moffett Field, California 94035
C. S. YENTSCH
Bigelow Laboratory, West Boothbay Harbor, Maine 04575

References and Notes

1. By the term "ocean color," we mean the spectrum of upwelling radiance just beneath the sea surface.
2. G. L. Clarke, G. C. Ewing, C. J. Lorenzen, *Science* **167**, 1119 (1970).
3. C. S. Yentsch, *Limnol. Oceanogr.* 7, 207 (1962); *Deep-Sea Res.* 7, 1 (1959); in *Proceedings of the Symposium on Remote Sensing in Marine Biology and Fisheries* (Texas A&M University, College Station, 1971), pp. 75–97.
4. For a general discussion of the ocean remote sensing problem and these interfering effects, see R. W. Austin, in *Optical Aspects of Oceanography*, N. G. Jerlov and E. Steeman Nielson, Eds. (Academic Press, New York, 1974), p. 494.
5. W. A. Hovis, M. L. Forman, L. R. Blaine, *Detection of Ocean Color Changes from High Altitude* (Publication X-652-73-371, National Aeronautics and Space Administration, Washington, D.C., 1973); W. A. Hovis and K. C. Leung, *Opt. Eng.* **16**, 153 (1977).
6. J. C. Arvesen, J. P. Millard, E. C. Weaver, *Astronaut. Acta* **18**, 229 (1973).
7. J. L. Mueller, "The influence of phytoplankton on ocean color spectra," thesis, Oregon State University (1973); *Appl. Opt.* **15**, 394 (1976).
8. H. R. Gordon, *Appl. Opt.* **15**, 1974 (1976); A. Morel and L. Prieur, *Limnol. Oceanogr.* **22**, 709 (1977).
9. R. C. Smith and K. S. Baker, *Limnol. Oceanogr.* **23**, 247 (1978); *ibid.*, p. 260; D. K. Clark, E. T. Baker, A. E. Strong, *Boundary-Layer Meteorol.*, in press; A. Morel and L. Prieur, in *Resultats de la Campagne CINECA 5 (Group Mediprod)* (Centre National pour l'Exploitation des Oceans, 1976), section 1-1-11.
10. S. Q. Duntley, R. W. Austin, W. H. Wilson, C. F. Edgerton, S. E. Moran, "Ocean color analysis" (final report under Naval Research Laboratory contract N00014-69-A-0200-6033 and NOAA grant 04-3-158-64, Reference 74-10, Scripps Institution of Oceanography, La Jolla, Calif., 1974).
11. The members of the CZCS NET are W. A. Hovis (sensor scientist), F. Anderson, J. R. Apel, R. W. Austin, D. K. Clark, H. R. Gordon, S. Z. El-Sayed, B. Sturm, R. C. Wrigley, and C. S. Yentsch.
12. H. R. Gordon, D. K. Clark, J. L. Mueller, W. A. Hovis, *Science* **210**, 63 (1980).
13. H. R. Gordon, *Appl. Opt.* **17**, 1631 (1978).
14. ——— and D. K. Clark, *Boundary-Layer Meteorol.*, in press.
15. The diffuse attenuation coefficient k has the property that $1/k$ is effectively the depth over which the pigment concentration is determined by the CZCS [See H. R. Gordon and R. W. McCluney, *Appl. Opt.* **14**, 413 (1975); H. R. Gordon, *ibid.* **17**, 1893 (1978)].
16. This research was supported under NASA contract NAS5-22963.

7 November 1979; revised 31 March 1980

Phytoplankton Pigments from the Nimbus-7 Coastal Zone Color Scanner: Comparisons with Surface Measurements

Abstract. *The removal of atmospheric effects from Nimbus-7 Coastal Zone Color Scanner (CZCS) images reveals eddy-like ocean turbidity patterns not apparent in the original calibrated images. Comparisons of the phytoplankton pigment concentrations derived from the corrected CZCS radiances with surface measurements agree to within less than 0.5 log* C, *where* C *is the sum of the concentrations of chlorophyll* a *plus phaeopigments* a *(in milligrams per cubic meter).*

The Nimbus-7 Coastal Zone Color Scanner (CZCS) was designed to measure the concentrations of phytoplankton pigments in the ocean (*1*). We report here initial comparisons between CZCS and surface determinations of pigment concentrations in the Gulf of Mexico. The data were collected during our first postlaunch experiment in November 1979.

The signal measured by the CZCS is related to the pigment concentration in the water through the scattering and absorption properties of the phytoplankton (*2*). Phytoplankton contain the photosynthetically active pigment chlorophyll *a* (Chl *a*), which is strongly absorbing near 443 nm. This absorption causes the solar radiation backscattered out of the ocean at 443 nm to decrease rapidly with increasing Chl *a* concentration. The Chl *a* absorption is much weaker at 520 and 550 nm. Therefore, an increase in Chl *a* causes the backscattered radiance to increase at these wavelengths as a result of the scattering associated with the phytoplankton [see figure 1 of (*1*)]. Thus, water that is poor in Chl *a* will appear a deep blue in sunlight, whereas water rich in Chl *a* will appear green.

A detrital pigment of Chl *a*, phaeopigments *a* (Phaeo *a*), possesses almost the same absorption spectrum as Chl *a*, and hence it cannot be separated from Chl *a* with the bands available on the CZCS. Because of this, only the sum of Chl *a* plus Phaeo *a* (henceforth indicated by *C*) can be estimated with this sensor (*3*). Usually, the Phaeo *a* concentration is lower by a factor of 5 to 10 than the Chl *a* concentration (*4*).

Following earlier investigators (*5*, *6*), we relate the pigment concentration to ratios of radiances at various wavelengths λ rather than to absolute radiances. This procedure has the advantage of partially compensating for the influence of other material in the water, such as nonorganic suspensoids, as well as the masking effects of the atmosphere discussed below. The algorithm relating ratios of radiances to C has been developed from measurements of upwelled subsurface spectral radiance L_w^λ and the associated pigment profiles from three areas: Southern California, Chesapeake Bay, and the Gulf of Mexico (including the Mississippi discharge region). Upwelled radiance measurements were made with a submersible scanning spectral radiometer with a 2° field of view and a 5-nm spectral resolution. Values of C, which ranged from 0.07 to 77 mg m^{-3}, were measured by means of the fluorometric technique (*7*). A regression analysis of these data (*4*) related C to the radiance ratios $R_1 = L_w^{443}/L_w^{550}$ and $R_2 = L_w^{520}/L_w^{550}$ through

$$\log C_i = \log a + b \log R_i, i = 1 \text{ or } 2 \quad (1)$$

where the coefficients $\log a$ and b, along with the coefficient of determination r^2

0036-8075/80/1003-0063$00.50/0

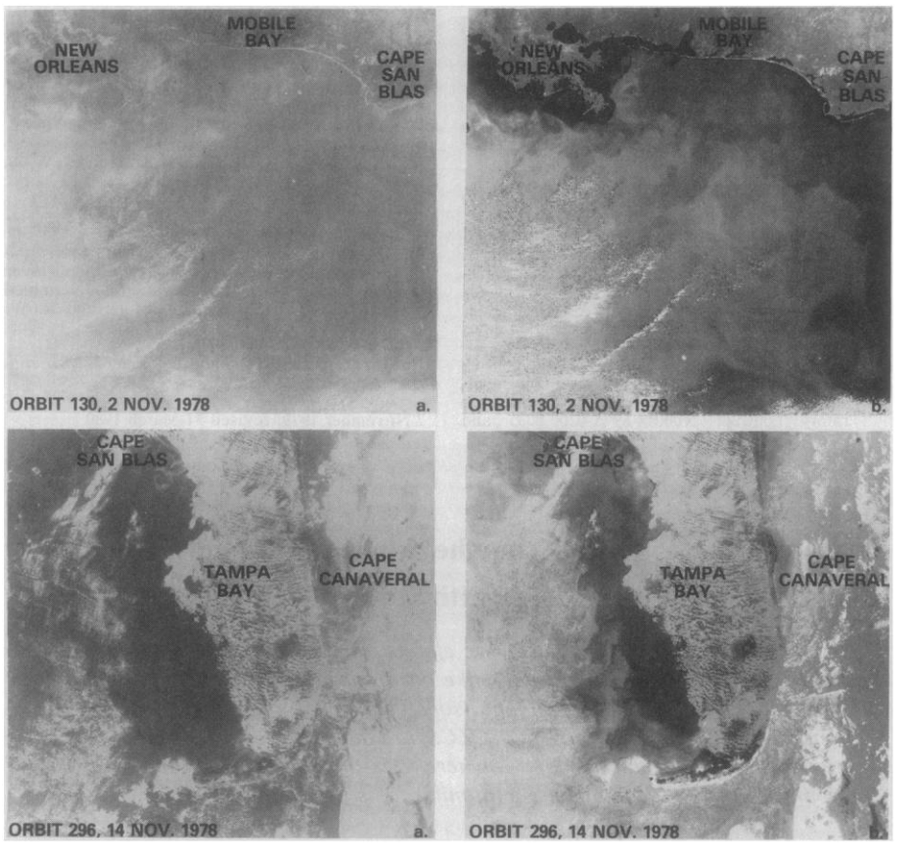

Fig. 1. Comparisons of calibrated CZCS channel 1 radiances L^{443} (a) with radiances L_W^{443} (b) corrected for atmospheric effects by means of Eq. 3 for Gulf of Mexico subscenes from Nimbus-7 orbits 130 and 296. Coefficients $\alpha(\lambda_1,\lambda_2)$ were derived from L_w^{λ} measurements made aboard the R.V. *Athena II* at a station just south of Mobile Bay in the extremely hazy orbit 130 scene and at a station just west of the cloud over Tampa Bay in the orbit 296 scene.

and the standard error of estimate S in $\log C$, are as follows. For R_1, the values of $\log a$, b, S, and r^2 are -0.297, -1.269, 0.173, and 0.978; for R_2, the corresponding values are -0.074, -3.975, 0.234, and 0.941. These data suggest that, even in the worst case, C can be estimated from radiance ratios to within a factor of 2.

The CZCS measured radiances cannot be directly used in Eq. 1 because scattering by the atmosphere between the sensor and the ocean contributes significantly to these values. Hovis and Leung (*5*) demonstrated this effect by noting the difference in the radiance spectrum observed from an aircraft when the altitude was increased from 0.91 to 14.9 km; in the blue region (near 400 nm) the radiance increased fivefold, whereas in the red (near 700 nm) the radiance increased by a factor of 2.5. It can be anticipated then that as much as 80 percent of the radiance detected at satellite altitudes could be due to atmospheric scattering. This atmospheric radiance is difficult to remove from CZCS imagery because of the component arising from aerosol scattering. The aerosols are highly variable (spatially and temporally) in concentration, composition, and size distribution.

The method we use here to remove the aerosol effects is based on a correction algorithm devised by Gordon (*8*). The

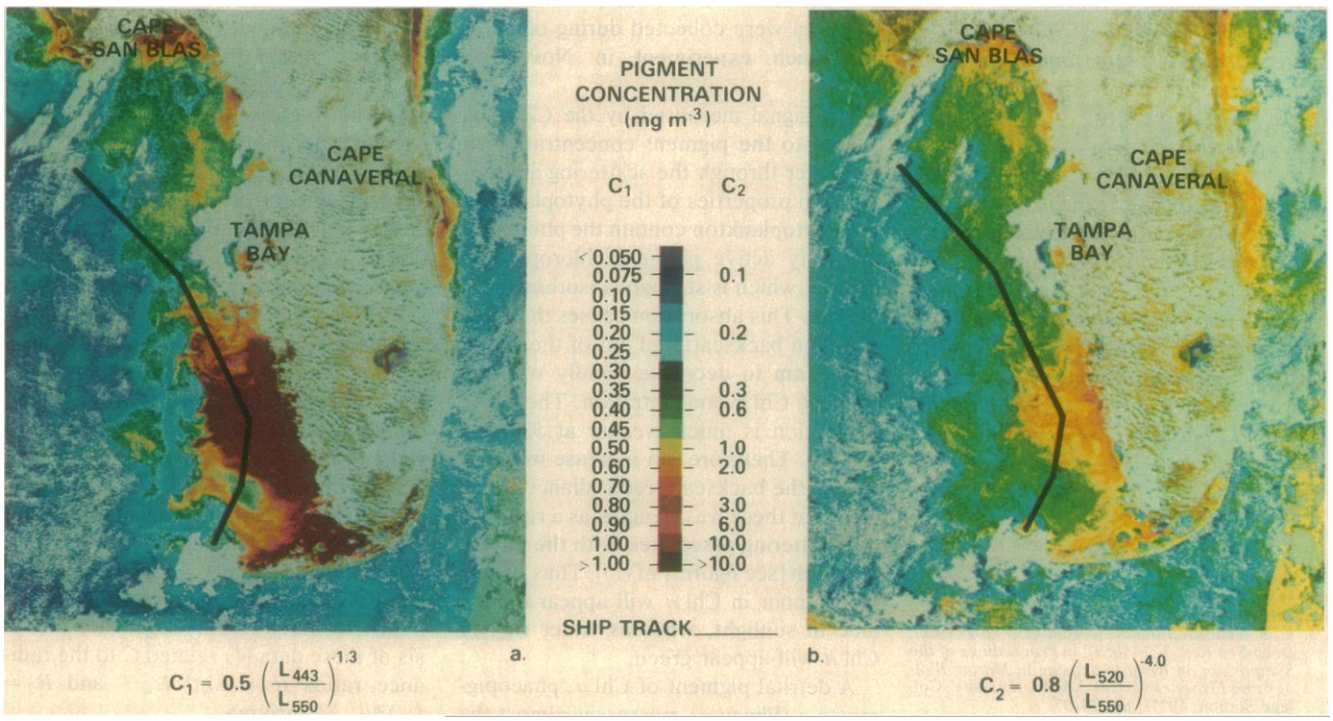

Fig. 2. Color-encoded concentrations of phytoplankton pigments C = (Chl α + Phaeo α) in the eastern Gulf of Mexico as derived from Nimbus-7 CZCS imagery on orbit 296: (a) is derived from R_1 and (b) is derived from R_2, using Eq. 1. The coefficients shown here are rounded to one decimal place, as derived from the Eq. 1 data. For notational convenience, we have replaced L_w^{λ} with L_{λ} (see Eq. 1). Land (brown) and clouds (white) were masked and superimposed on the image as explained in (*1*). The track shown was traversed by the R.V. *Athena II* on 13 and 14 November 1978 (see Fig. 3).

basic idea has two parts. First, to an excellent approximation, the total radiance L^λ observed by the sensor at wavelength λ can be partitioned into that due to Rayleigh-scattering $L_R{}^\lambda$, that due to aerosol-scattering $L_A{}^\lambda$, and the radiance backscattered out of the ocean $L_W{}^\lambda$ as transmitted through the atmosphere; that is,

$$L^\lambda = L_R{}^\lambda + L_A{}^\lambda + t^\lambda L_W{}^\lambda \quad (2)$$

where t^λ is the diffuse transmittance of the atmosphere (*9*). Skylight reflected from the surface toward the sensor is implicitly included in $L_R{}^\lambda$ and $L_A{}^\lambda$.

Second, if the aerosol-scattering phase function is independent of λ, then $L_A{}^\lambda$ at one wavelength will be approximately proportional to that at another wavelength. Thus, if we apply Eq. 2 at two wavelengths λ_1 and λ_2, we obtain

$$t^{\lambda_2} L_W{}^{\lambda_2} = L^{\lambda_2} - L_R{}^{\lambda_2} - \alpha(\lambda_1,\lambda_2)\,[L^{\lambda_1} - L_R{}^{\lambda_1} - t^{\lambda_1} L_W{}^{\lambda_1}] \quad (3)$$

where $\alpha(\lambda_1,\lambda_2)$ is a constant which can be related to the optical properties of the aerosol through the single scattering approximation (*10*). If λ_1 is chosen such that $L_W{}^{\lambda_1} \approx 0$, then $L_W{}^{\lambda_2}$ can be determined for any λ_2, provided $\alpha(\lambda_1,\lambda_2)$ is known. Of the CZCS bands, 670 nm is the most suitable except in regions of very high turbidity. In this report $\alpha(\lambda_1,\lambda_2)$ is determined from Eq. 3 by direct in situ measurement of $L_W{}^\lambda$ at one location in the image, and then these values are used throughout the entire image.

We now present the results of applying these algorithms to imagery of the Gulf of Mexico from Nimbus-7 orbits 130 and 296. The availability of surface measurements was the only criterion used to select the imagery. The image from orbit 130 provides a very demanding test of the atmospheric correction algorithm because of the strong horizontal structure in the rather intense haze. The image from orbit 296 represents a more normal atmospheric condition.

Figure 1 compares the corrected radiance (b) with the calibrated radiance (a) at 443 nm for Gulf of Mexico subscenes from orbit 130 (Mississippi Gulf coast) and orbit 296 (Florida Gulf coast). We obtained corrected images by applying Eq. 3 to the calibrated radiance after determining $\alpha(\lambda_1,\lambda_2)$ from simultaneous shipboard measurements of $L_W{}^\lambda$ at stations just south of Mobile Bay and just west of Tampa Bay for orbits 130 and 296, respectively. The corrected images reveal an impressive series of eddy-like structures which could not be distinguished from atmospheric variations in the original images. Note in particular that the corrected image from orbit 130 shows little trace of the haze structure which dominated the original image [see figure 2 of (*1*)]; this result indicates that $\alpha(\lambda_1,\lambda_2)$ is nearly constant over large portions of the image.

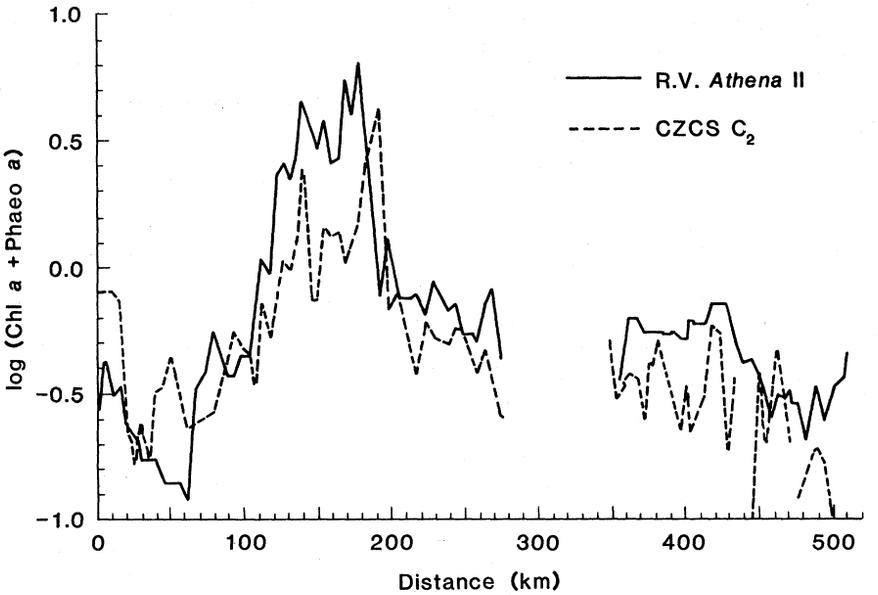

Fig. 3. Values of C = (Chl a + Phaeo a) (in milligrams per cubic meter) from Fig. 2 (14 November 1978) compared with a track line of concentrations measured aboard the R.V. *Athena II* on 13 and 14 November 1978. The track line is superimposed on Fig. 2, and distance (above) runs from south to north. The estimated CZCS data have been subsampled to coincide with the ship samples for comparison.

We now turn to the determination of pigment concentrations from the corrected radiances. Figure 2 gives the distribution of pigment concentrations for the orbit 296 subscene determined from Eq. 1. At low pigment concentrations, $L_W{}^{443}$ varies strongly with C, and hence R_1 is very sensitive to small changes in C at low concentration. Conversely, at high concentrations $L_W{}^{443}$ becomes very small, necessitating an unrealistically accurate atmospheric correction for its retrieval from L^{443}. Because of this, R_1 is useful only for pigment concentrations lower than 0.6 mg m^{-3} (*4*).

Superimposed on Figure 2 is the track of the R.V. *Athena II* from 1500 hours on 13 November to 2000 hours on 14 November 1978 (29 hours). At the time of the CZCS overpass, the ship was occupying a station due west of Tampa Bay (station 10). We determined pigment concentration along the ship track from the CZCS using R_2, and it is compared with the shipboard measurements of C in Fig. 3. The general features of the shipboard measurements are well reproduced in the CZCS estimations (note, in particular, the high pigment feature between 100 and 200 km). However, the high-frequency variability of the CZCS data is much larger in amplitude than the corresponding ship measurements. Moreover, were the CZCS data represented at full resolution (1 km), the CZCS chlorophyll estimates would be substantially noisier in appearance. High-frequency fluctuations are particularly characteristic of the radiance ratio R_2 as a direct result of the relatively coarse digitization increment of the Nimbus-7 CZCS.

The pigment concentrations measured by the CZCS seem to be consistently lower than the ship measurements (Fig. 3), which is probably due to a combination of subpixel structure, water motion, and navigation errors (*11*). Comparison of Figs. 2 and 3 suggests that a movement of the high pigment region only 10 to 12 km westward between the times of the ship and the CZCS measurements (about 12 hours) would bring the observed and derived concentrations into much better agreement. Even so, Fig. 3 indicates that the CZCS Nimbus experiment team's goal of estimating pigment concentrations to within 0.5 log C has been met by the present system.

Since shipboard measurements of $L_W{}^\lambda$ at one position in each image were used to determine $\alpha(\lambda, 670)$, it is of interest to know how well C could be estimated without these measurements. In the absence of surface measurements of any kind, one must locate an area of the image where C is obviously very small and then solve (*3*) for $\alpha(\lambda, 670)$, using typical

values of clear water L_W^λ measured at other times for approximately the same solar elevation. When this is done for station 10, with an area south of Key West used as representative of clear water, the resulting derived pigment concentrations from R_1 and R_2 are, respectively, 0.21 and 0.33 mg m^{-3}. If the values of L_W^λ measured aboard the R.V. *Athena II* at station 10 are used to estimate $\alpha(\lambda, 670)$, the derived concentrations are 0.33 and 0.26 mg m^{-3}, respectively. The measured pigment concentration at station 10 was 0.36 mg m^{-3}. Clearly, this technique shows considerable promise for estimating pigment concentrations in regions where surface measurements are not available.

The limited results presented here suggest that maps of phytoplankton pigment concentration can presently be derived from CZCS imagery to better than 0.5 log C. Furthermore, the corrected CZCS imagery reveals circulation patterns heretofore unobserved in satellite imagery of the Gulf of Mexico. A CZCS-type system can be of considerable value in augmenting the study of complex coastal circulation processes and ecology.

HOWARD R. GORDON
Department of Physics,
University of Miami,
Coral Gables, Florida 33124
DENNIS K. CLARK
National Environmental Satellite Service, National Oceanic and Atmospheric Administration, Washington, D.C. 20233
JAMES L. MUELLER
Laboratory for Atmospheric Sciences, National Aeronautics and Space Administration, Goddard Space Flight Center, Greenbelt, Maryland 20771
WARREN A. HOVIS
National Environmental Satellite Service, National Oceanic and Atmospheric Administration

References and Notes

1. W. A. Hovis *et al.*, *Science* **210**, 60 (1980).
2. A. Morel and L. Prieur, *Limnol. Oceanogr.* **22**, 709 (1977).
3. In addition to the absorption effects of Chl *a* and Phaeo *a*, the accessory pigments chlorophyll *c* and carotenoids also contribute to the total absorbance within the 443-nm band. These effects are assumed to covary with *C*.
4. H. R. Gordon and D. K. Clark, *Boundary-Layer Meteorol.*, in press.
5. W. A. Hovis and K. C. Leung, *Opt. Eng.* **16**, 157 (1977).
6. G. L. Clarke, G. C. Ewing, C. J. Lorenzen, *Science* **167**, 1119 (1970); J. C. Arvesen, J. P. Millard, E. C. Weaver, *Astronaut. Acta* **18**, 229 (1973).
7. C. S. Yentsch and D. W. Menzel, *Deep-Sea Res.* **10**, 221 (1963); O. Holm-Hansen, C. J. Lorenzen, R. W. Holmes, J. D. H. Strickland, *J. Cons. Cons. Perm. Int. Explor. Mer* **30**, 3 (1965).
8. H. R. Gordon, *Appl. Opt.* **17**, 1631 (1978).
9. ———, *ibid.* **15**, 1974 (1976).
10. Specifically, $\alpha(\lambda_1,\lambda_2)$ is equal to the product of the ratios of the aerosol optical thicknesses, the single scattering albedos, and the extraterrestrial solar irradiances (after accounting for ozone absorption) at the two wavelengths in question.
11. The ship track and station 10 location are probably navigated to no better than 12 pixels with respect to the imagery. A more accurate location for station 10 could result in a more accurate atmospheric correction.
12. We acknowledge the assistance of D. Ball of Computer Sciences Corporation in the production of the results and figures presented in this report. We also thank Dr. A. E. Strong, Dr. E. T. Baker, H. Stumpf, R. Comeyne, E. King, J. Kapsch, R. Hill, and S. Roman of the National Oceanic and Atmospheric Administration; Dr. D. Kiefer and J. SooHoo of the University of Southern California; Dr. W. Broenkow of San Jose State University; and the captain and crew of the R.V. *Athena II* for their indispensable assistance in the collection of the in situ oceanographic data. One of us (H.R.G.) was supported by NASA contract NAS 5-22963.

7 November 1979; revised 31 March 1980

Atmospheric Carbon Dioxide, the Southern Oscillation, and the Weak 1975 El Niño

Abstract. *The observed rate of change of the atmospheric carbon dioxide concentration at the South Pole, Fanning Island, Hawaii, and ocean weather station P correlates with an index of the southern oscillation and with El Niño occurrences. There are changes at all four stations that seem to be in response to the weak 1975 El Niño. Thus, even poorly developed El Niño events may affect the atmospheric carbon dioxide concentration.*

The rate of change of the atmospheric concentration of CO_2 at the South Pole and at Mauna Loa, Hawaii, has been shown to be significantly correlated with a southern oscillation index (SOI) (*1*). The southern oscillation is a large-scale atmospheric and hydrospheric fluctuation centered in the equatorial Pacific Ocean and involving wind strengths, ocean currents, and sea-surface temperatures (*2*). It has a variable period, averaging approximately 4 years. El Niño occurrences are probably the most spectacular of the phenomena associated with the southern oscillation. Changes in atmospheric CO_2 have been observed that correspond to the El Niño's of 1965, 1969, and 1972 (*3*).

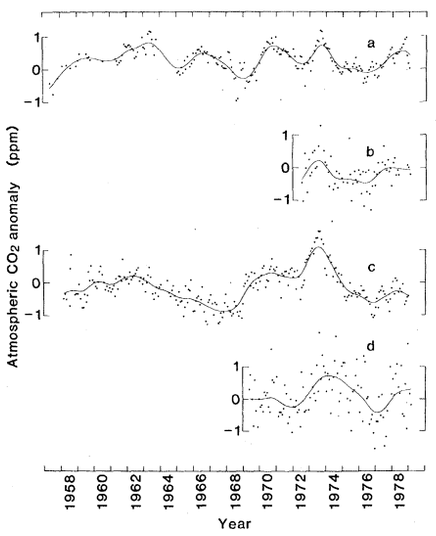

Fig. 1. Atmospheric CO_2 anomalies at (a) the South Pole, (b) Fanning Island (4°N), (c) Mauna Loa, Hawaii (20°N), and (d) Canadian ocean weather station P (50°N). The anomaly curves are spline fits to data from which an average seasonal effect and a smooth trend have been removed.

Correlations between SOI and the rate of change of atmospheric CO_2 at Fanning Island, near the equator (4°N), and at ocean weather station P, off the Canadian west coast (50°N), as reported here, tend to confirm the association. There are changes at all four stations that correspond to the 1972 and 1976 El Niño events, and, seemingly, to the weak 1975 El Niño as well.

The El Niño of 1975 was so weak that it probably would not have been recognized as an El Niño, were it not so well studied (*4*, *5*). El Niño refers to an oceanic and meteorological disturbance in the Peruvian coastal area apparently caused by an invasion of warm, nutrient-poor surface water into an area normally occupied by colder, more nutrient-rich water of upwelling origin. A fully developed El Niño is characterized by torrential rains in the normally arid coastal region and disruption of the large anchovy fishery as the fish seek colder, more nutrient-rich water.

The prediction of the 1975 El Niño by Quinn (*6*) led to the El Niño Watch Expedition, which systematically collected oceanographic data in the region west of the South American coast, from 5°N to 15°S. In February and March 1975, a thin tongue (10 to 25 m thick) of low-salinity, warm, nutrient-poor water extended south across the equator eastward of the Galápagos Islands, but the Peruvian coastal region and its fishery were essentially undisturbed. The invasion of warm surface water was short-lived; by May, conditions had returned to near normal. Wyrtki *et al.* (*4*) have suggested that the term El Niño be reserved for the spec-

0036-8075/80/1003-0066$00.50/0